Design: We identified 101 cases of pure DCIS and 225 cases of DCIS with co-existing IDC at University of Rochester Medical Center between 1997 and 2008. The clinical (patient age) and pathological (tumor size and nuclear grade) features were recorded, tissue microarray from these cases were constructed, and immunohistochemical (IHC) analyses were performed for ER, PR, AR (androgen receptor), HER2, Ki67, IMP3 (Insulin-like growth factor II mRNA-binding protein 3), Bcl2, Cox2 and Cyclin D1. ER, PR and AR were scored positive with Allred scores ≥3; HER2 was scored according to 2007 ASCO/CAP guidelines; Ki67 was scored positive with ≥15% of nuclear staining; any strong cytoplasmic staining was considered positive for IMP3; ≥10% strong nuclear staining was considered as positive for Cyclin D1, Bcl2; and ≥25% cytoplasmic stain was defined as positive for Cox2.

Results: Comparison between these two groups showed only tumor size, nuclear grade, and IMP3 with significant difference. However, when we compared different subgroups by patient age, tumor size, nuclear grade, and expression of ER/PR, HER2 and Ki67, significant difference were observed for all these factors in different subgroups. The higher expressions of ER, PR, AR, HER2, Cyclin D1 and Cox2 were associated with pure DCIS; while higher expressions of Ki67, IMP3 and Bcl2 were observed in DCIS with co-exisiting IDC.

	Age (y)	Size (cm)	Nuclear Grade	ER/PR	HER2	Ki67
Expression levels in DCIS > IDC						
ER+, PR+	<40		3			
AR+		>4.0	3			
HER2+	>60			ER-/PR-		
Cyclin D1+			3	ER-/PR-	HER2+	>15%
Cox 2+					HER2-	
Expression levels in DCIS < IDC						
Ki67+	40-60		3		HER2-	
IMP3+		>4.0				
Bcl2+				ER+/PR+		

Conclusions: Breast carcinoma is a heterogeneous group of tumors, different biomarkers may play critical roles in cancer progression of different subgroups.

317 Stromal Cells in Phyllodes Tumors of Breast Exhibit Stem Cell Marker Expression

Y Zhang, E Chung, KA Toy, LJ Pierce, CG Kleer. UC Davis Medical Center, Sacramento, CA; University of Michigan, Ann Arbor, MI.

Background: Phyllodes tumors (PT) of breast are fibroepithelial neoplasms with stromal hypercelullarity, which is the basis for the diagnosis of benign, borderline and malignant. The histologic diagnosis of PT is often difficult, and the pathological features may not always predict clinical behavior. Previous studies suggest that EZH2 epigenetically regulates cell-type identity and cellular differentiation. We hypothesized that in PT, EZH2 and the stem cell marker ALDH1 may be expressed in stromal cells and associated with their degree of differentiation.

Design: Fourty-one PTs were histologically classified following WHO criteria, and blinded to outcome. Immunohistochemistry for EZH2 and ALDH1 was routinely performed on formalin-fixed, paraffin-embedded whole tissue sections. The percentage of ALDH1 expressing stromal and epithelial cells was recorded. A low or high EZH2 expression was identified based on a cutoff of 10% positive staining cells.

Results: Of the 41 PTs, 25 (61%) were benign, 8 (19.5%) borderline, and 8 (19.5%) malignant. EZH2 expression was low and rare in the epithelial cells, but significantly overexpressed in the stromal cells of borderline and malignant PT (4 of 8, 50% of each, $p<0.005$). ALDH1 was exclusively expressed in the stromal cells of PT, and significantly associated with the histological classification. ALDH1 positive cells were present in 40% of benign PT, 75% of borderline and 75% of malignant PT respectively ($p<0.005$).

Conclusions: EZH2 expression in PT may be helpful to distinguish benign from borderline and malignant tumors in challenging cases. Our data suggest that the stromal cells in PT exhibit a mesenchymal stem cell component, which increases with the degree of malignancy.

1586 Predicting 5-Year Recurrence of Ductal Carcinoma In Situ (DCIS) Following Initial Breast Conserving Surgery and Radiation Therapy

CP Kragel, S Wei. University of Alabama at Birmingham, Birmingham, AL.

Background: A large number of previous studies have identified various clinicopathologic factors significantly associated with local recurrence (LR) for DCIS. However, the LR rate has been greatly reduced since breast-conserving surgery (BCS) with radiation therapy (RT) became a standard treatment option in women with localized DCIS. Yet, there is still a benefit to identifying patients at lower risk for LR in order to avoid overtreatment. In this study, we sought to establish factors significantly associated with LR and to examine the utility of the recently published Memorial Sloan-Kettering (MSK) nomogram in predicting LR rates in patients with DCIS after BCS and RT.

Design: The Surgical Pathology files of the authors' institution were searched to identify patients with DCIS who underwent BCS and subsequent RT from 2003-2007. Those with coexisting invasive carcinoma or receiving mastectomies following BCS with positive margins were excluded. The odds ratios (OR) were calculated, and Fisher Exact Probability or t test was utilized for statistical analysis, when appropriate. The clinicopathologic factors populated the MSK DCIS nomogram.

Results: A total of 31 cases meeting the inclusion criteria were identified in the study period, of which only 4 patients (13%) had LR within 5 years, 3 with DCIS and 1 with invasive carcinoma. While the presence of necrosis in DCIS showed the highest odds ratio for LR, univariate analysis failed to identify any of the clinicopathologic factors examined significantly associated with LR. Further, there was no clear association between the MSK nomogram-predicted and observed 5-year LR rates. The mean probability of LR was 3.75% in the recurrence group and 2.81% in the non-recurrence group (p=0.16).

Univariate Analysis of Clinicopathologic Factors

Variables	OR	95% CI	p-value
No. of re-excisions (1 vs. 2&3)	1.1	[0.1, 11.8]	1.0
Family history of cancer	0.4	[0.03, 3.9]	0.4
Endocrine therapy	2.1	[0.2, 22.5]	0.6
ER+	0.4	[0.04, 3.0]	0.3
PR+	2.4	[0.2, 25.9]	0.5
Nuclear grade (3 vs. 1&2)	2.9	[0.3, 24.3]	0.3
Necrosis	5.1	[0.5, 55.9]	0.2
Close margins (2 mm or less)	2.6	[0.2, 33.2]	0.5

Conclusions: As management of localized DCIS has become more standardized to include BCS and RT, it may become more difficult to reliably predict 5-year LR risk. Large-scaled studies may be needed to accurately evaluate the DCIS recurrence risk in patients who received standardized therapy to assist clinical decision making in pursuit of individualized medicine.

Cardiovascular

318 Preclinical Evaluation of Plaque Morphology and Development by Flat-Panel Computed Tomography

I Aboshady, LM Buja. Texas Heart Institute, Houston, TX; University of Texas HSC, Houston, TX.

Background: Current multidetector computed tomography (MDCT) imaging of plaque components within lesions will require additional improvement to the instrumentation in order to accurately predict their vulnerability. We have previously shown in an acute pilot study that Flat-panel computed tomography (FpCT) provides better spatial resolution than 64-MDCT and better assesses plaque components *in vivo* in animal aortas similar in size to human coronary arteries. In this phase, we quantitatively evaluated the maximum capabilities and limitations of FpCT in longitudinal studies of plaque development as correlated to histopathology as a gold standard.

Design: The commercially available amorphous silicon fluoroscopic FpCT x-ray detectors offer 200μ native resolution. With an automated tool; multiplanar reformatted images were created perpendicular to the center line of the aorta along its entire imaged length. Lesions in 184 aortic histology sections from 6 WHHL rabbits and 30 NZW hyperlipidemic rabbits were quantitatively compared with 64-CT (image thickness, 0.625 mm) and FpCT (image thickness, 0.150 mm) images. In the long-term phase of the study, rabbits received a high-fat diet (0.5% cholesterol) and angiotensin II (0.4 $\mu g\ kg^{1}\ min^{1}$, through SC osmotic pumps) for 6 months. Lesions are monitored and correlated through monthly serial scanning sessions over 6 months.

Results: FpCT was more sensitive in detecting eccentric lesions (42% vs. 0%; P=0.000). In detecting plaques with ≤10% lipid (low-attenuation foci), FpCT was more sensitive than 64-CT (24% vs. 0.7%; P<0.00) and had a greater AUC (0.6 vs. 0.5; P<0.006). Additionally, FpCT was more sensitive (65% vs. 0%; P<0.00) in detecting plaques with ≤5% calcium (high-attenuation foci) but not in detecting branch points. Both FpCT and histology could detect low-attenuation foci as small as 0.3 mm, whereas 64-CT could detect only low-attenuation foci ≥1.5 mm in diameter. Of the 48 lesions classified to AHA criteria as type II by histology, 42 were also classified as type II by FpCT and 35 by 64-CT. FpCT was significantly more sensitive than 64-CT in detecting all types.

Conclusions: The study confirms our pilot study data that FpCT seems to have more potential in quantitative screening for low-risk small atherosclerotic lesions than MDCT in a rabbit model of atherosclerosis. FpCT have also the capacity for quantitatively assessment the development of calcific and lipid components of atherosclerotic plaque.

319 Detection of Soluble Lectin-Like Oxidized Receptor (sLOX-1) as a Biomarker To Predict Sickle Cell Disease Vasculopathy

M Chen, X Lin, H Archibald, R Green. UC Davis Medical Center, Sacramento, CA.

Background: Sickle cell disease (SCD) crisis is associated with significant morbidity and mortality due to vascular occlusion. Lectin-like oxidized low-density lipoprotein receptor-1 (LOX-1) is identified as a major endothelial receptor for oxidized low-density lipoprotein (ox-LDL) as well as aged erythrocytes. Enhanced expression of LOX-1 is implicated in atherosclerosis, inflammation and diabetic vasculopathy. The pathogenesis of SCD vasculopathy mechanistically resembles atherosclerosis. The purpose of this study is to investigate the role of LOX-1 as a biomarker to predict SCD vasculopathy.

Design: We analyzed LOX-1 gene expression by qPCR in human coronary endothelial cells following static incubation with sickle RBCs. We studied in vivo LOX-1 expression in autopsy SCD patient's vasculatures by immunohistochemistry. We measured circulating soluble LOX-1 (sLOX-1) concentrations by sandwich ELISA in the plasma of SCD patients under sickle cell crisis compared with steady-state.

Results: LOX-1 mediated binding and internalization of sickle RBCs in endothelial cells was inhibited by pre-incubation with Ox-LDL.

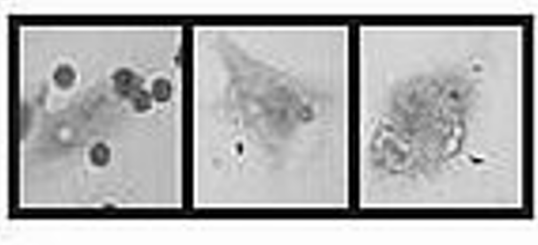

LOX-1 gene expression in human endothelial cells was significantly increased by incubation with sickle RBCs. Upregulation was detected after 1 hour of incubation,

and reached a peak after 6 hours. We studied 48 SCD (Hb SS) patients (26 female, 22 male); vs 17 healthy (Hb AA) control subjects (12 female, 5 male). The SCD cohort comprised pediatric and adult patients in steady-state (33 patients) and vaso-occlusive crisis (VOC; 15 patients). The concentration of circulating sLOX-1 protein in plasma of sickle cell disease patients (mean: 3.09±2.51 ng/mL; range 0.3 – 11.3 ng/mL) was significantly higher (p=0.006) than in control healthy subjects (mean: 1.27±0.79 ng/mL). In 15 SCD patients in VOC, the sLOX-1 concentrations were elevated (mean: 3.70±2.33 ng/mL).

Conclusions: We demonstrate that SCD erythrocytes can induce endothelial LOX-1 expression, and the circulating sLOX-1 levels are elevated in SCD patients in sickle cell crisis. Studies of sLOX-1 in SCD may provide new insights into risk stratification, and may lead to novel therapeutic strategies for sickle cell patients with acute vascular complications.

320 Correlations of Donor Specific Antibodies and Acute Rejection with T Cell Subtype Infiltrates in Endomyocardial Biopsies

R Frank, M Kamoun, P Lal. Hospital of the University of Pennsylvania, Philadelphia, PA.

Background: Acute antibody-mediated rejection (AMR) is a major complication after heart transplantation, posing a significant risk for allograft failure, cardiac allograft vasculopathy, and poor survival. While the inflammatory mileu of cellular rejection and Quilty lesions are well-known, the immunologic components AMR are not well understood. Our aim was to better define the immunophenotype of infiltrating lymphocytes in biopsies with AMR, specifically in relation to donor specific antibodies to HLA class I, II, or both.

Design: We performed a retrospective analysis of cardiac transplant patients with acute cellular rejection (ACR) who had concurrent endomyocardial biopsies (EMB), DSA measurements and immunofluorescence for C4d at our institution (2005-2011). DSA were evaluated against HLA class I and class II specificities pre and post transplant using flow cytometry and/or Luminex bead assays. ACR and AMR were based on the ISHLT 2005 report, including diffuse interstitial capillary C4d and DSA presence. Immunohistochemical analysis for CD3, CD4, CD8 and CD79a was performed using standard immunohistochemical protocols on one formalin-fixed paraffin embedded EMB from each patient. The number of lymphocytes expressing each protein was enumerated microscopically at 400X. Ratios of T:B cells and CD4:CD8 T cells were then calculated for each EMB.

Results: 76 cardiac transplant patients who had pre and post transplant DSA measurements were analyzed. Of these 76 patients, 37 had DSA against either HLA class I, class II, or both. Of patients with DSA, the average CD4:CD8 ratio in the EMB was 0.80 while those with only acute cellular rejection had a CD4:CD8 ratio of 1.49. Interestingly, the T:B cell ratio in patients with and without DSA was 5.7 and 5.5, respectively.

Conclusions: Cardiac transplant patients with AMR and ACR have more cytotoxic T cells than helper T cells in the EMB lymphocytic infiltrate compared with patients having only ACR. The biologic significance of this ratio is currently unknown but may aid in diagnosis and treatment of AMR. The T cell ratios did not differ by having DSA to class I, II, or both. The inflammatory infiltrate T:B cell ratio was similar in patients both with and without AMR.

321 Loss of PRKAR1A Expression in Carney Complex-Associated Versus Nonsyndromic Cardiac Myxomas: Immunohistochemical and Molecular Analysis of 112 Cases

BT Larsen, MC Castonguay, NS Kip, BR Kipp, JJ Maleszewski. Mayo Clinic, Rochester, MN.

Background: Cardiac myxoma usually presents in a sporadic, nonsyndromic fashion as a solitary mass, but occasionally occurs as part of the Carney complex (CNC). Two-thirds of CNC-associated myxomas exhibit mutations in *PRKAR1A*, the gene encoding the cAMP-dependent protein kinase type Iα regulatory subunit. *PRKAR1A* mutations occur in both familial and nonfamilial forms of CNC, but whether these mutations occur in nonsyndromic cardiac myxomas is unknown.

Design: All cardiac myxomas (1993-2011) were retrieved from our institutional pathology files, and clinical and pathologic findings were reviewed. Immunohistochemistry was performed with an antibody directed against PRKAR1A protein, and staining of myxoma cells was graded semiquantitatively. Bi-directional Sanger sequencing was also performed to test for the presence of mutations in all coding regions and intron/exon boundaries of the *PRKAR1A* gene.

Results: Among 112 patients, 9 patients with CNC were identified (mean age 28 yrs, range 12-45, 7 female). In these patients, cardiac myxomas originated in diverse locations (left atrium 52%, right atrium, right ventricle, and left ventricle each 16%) and were multiple in 5 cases. Additional features of CNC included family history of cardiac myxomas (5 cases), Cushing syndrome (3), ephelides (3), cutaneous myxomas (2), blue nevi (1), and calcifying testicular tumors (1). Mutational analysis has been completed in 2 CNC cases, confirming *PRKAR1A* mutations in each (G891A and R228X). The remaining 103 patients (mean age 62 yrs, range 18-92, 65 female) presented with a solitary cardiac myxoma (left atrium 87%, right atrium 11%, right ventricle 2%), without other features of CNC. From all patients, 118 cardiac myxomas were available for review. Immunostaining for PRKAR1A was absent in all CNC-associated cardiac myxomas, consistent with loss of PRKAR1A expression. Unexpectedly, PRKAR1A staining was also absent in 30% of nonsyndromic myxomas and diminished (<50% of myxoma cells positive) in an additional 2% of cases, but was preserved in cardiomyocytes, indicating that PRKAR1A is selectively lost in many nonsyndromic tumors. Complete mutational analysis of the non-CNC cohort is ongoing.

Conclusions: Loss of PRKAR1A expression occurs not only in CNC-associated cardiac myxomas, but also in nearly one-third of sporadic nonsyndromic tumors. *PRKAR1A* mutations and/or alterations in its protein product may play a role in nonsyndromic cardiac myxomagenesis.

322 The Biventricular Form of Arrhythmogenic Cardiomyopathy Is the Most frequent Morphologic Substrate of Juvenile Sudden Cardiac Death in Sports

M Mancini, CRT di Gioia, R Ierino, C Preziuso, C D'Ovidio, P Gallo, V Petrozza, C Giordano, G d'Amati. Sapienza, University of Rome, Rome, Italy; "G. D'Annunzio" University, Chieti, Italy.

Background: Juvenile cardiac sudden death (SD) can occur during sport activity, either recreational or competitive. Physical effort triggers sudden death in athletes affected by cardiac disease presisposing to life-threatening arrhythmias. Thus, a more specific understanding of the cardiac substrates of SD is helpful to guide prevention programs. Our aim was to investigate the morphologic substrates of exertional juvenile cardiac SD.

Design: We reviewed 266 consecutive cases of juvenile sudden cardiac death (≥1 yr.≤40 yrs.) referred to our Department from January 2000 to May 2012. Accurate gross description was available for each heart; the diagnosis was based on macroscopic features and systematic microscopic analysis of the coronary arteries, valves and myocardium based on a detailed study protocol. According to the circumstances, sudden deaths were divided into: i) events occurring during or immediately after sports; ii) events at rest or during normal daily activities.

Results: Thirty-seven (14%) deaths occurred during sports (6 competitive and 31 non competitive athletes). There were 33 males and 4 females, with a mean age of 24.6 yrs. (range 10-38 yrs.). The sport most frequently involved was soccer (51% of cases). Toxicology was available in 24/37 cases, and was positive in one (cannabinoids). The most frequent cause of death was arrhythmogenic cardiomyopathy (ACM, 7/37,19%). All ACM cases showed a biventricular pattern, often with prevalent involvement of the left ventricle (2/7, 29%). Other morphologic substrates were atherosclerotic coronary artery disease (CAD, 4/37, 11%), congenital valvular disease (4/37,11%), congenital anomalies of coronary arteries (3/37, 8%), hypertrophic cardiomyopathy (HCM, 3/37, 8%), conduction tissue disease (2/37, 5%), myocarditis (2/37 5%), coronary artery vasculitis (1/37,3%), cardiac amartoma (1/37 3%). In 10/37 cases (27%) the findings were non-specific left ventricular hypertrophy (11%) or structurally normal heart (16%).

Conclusions: According to our results, the biventricular form of ACM is the most frequent morphologic substrate of juvenile sudden cardiac death in sports. In one third of cases the fibro-fatty myocardial replacement is limited to mild changes almost exclusively affecting the left ventricle.

323 Pediatric Marfan Syndrome Associated Aortic Disease: A Clinical-Morphologic Review

DV Miller, LK Erickson, AT Yetman, SC Menon. University of Utah - Primary Children's Medical Center, Salt Lake City, UT.

Background: Marfan syndrome is an autosomal dominant inherited connective tissue disorder with a population prevalence of 0.4-0.6%. Its primary manifestations include pectus deformities, ocular lens dislocation, arachnodactyly, mitral valve prolapse and aortic root dilatation. Complications of aortic root dilatation are the most feared and while early dilatation is common in childhood, the rate of progression is variable. Surgical aortic root repair is most often performed in adulthood, but may be necessary during childhood as well. This report describes the clinical features of Marfan patients undergoing aortic surgery at a children's hospital and the histomorphologic features of their aortic tissue.

Design: Patients with Marfan syndrome (on the basis of Ghent nosology and/or *FBN1* mutation) undergoing aortic root replacement at Primary Children's Medical Center were identified in medical record databases. Pertinent clinical data were abstracted from charts and pathologic specimens from these patients (including elastic-stained aortic tissue sections) were systematically reviewed.

Results: Eleven Marfan syndrome patients underwent root replacement during the interval from 2000 to 2012. Six were male, all were white (with two ethnic Hispanics), and ages at surgery ranged from 2 to 22 (mean 15) years. The mean interval from Marfan syndrome diagnosis to surgery was 5 months for those with aneurysm as the presenting sign and 72 months for patients diagnosed on the basis of other findings. As expected, all patients showed maximal aortic dilatation at the sinus level (mean 48 mm). The sinotubular junction (mean 31 mm) and ascending aorta (mean28 mm) were also enlarged in all patients. All repairs were elective and used valve sparing techniques, however 2 patients subsequently needed valve replacement. Histologically, only one case showed normal medial architecture (the 2-year-old). The others showed either "cystic" medial degeneration (1 mild, 4 moderate) or diffuse pattern medial degeneration (2 mild, 3 moderate). There was no histologic evidence of dissection.

Conclusions: This series refines the focus of Marfan related aortic disease in pediatric patients. As with adults, the sinus portion of the aorta is most severely affected. The aneurysms (by definition) showed aggressive enlargement and all but one showed corresponding medial histopathologic changes. The diffuse pattern of medial degeneration was seen in at least one patient with confirmed *FBN1* mutation.

324 Surgical Pathology of Ascending Aortic Aneurysms: Are There Clinical Correlates of Elastic Fragmentation of the Tunica Media?

S Rizzo, M Martin, R Razzolini, G Gerosa, G Thiene, C Basso. University of Padua, Padua, Italy.

Background: To evaluate: a) the prevalence of the different etiologies of ascending aorta aneurysms (AAA); b) the correlation between aortic diameters and elastic fragmentation score; c) whether aortic wall compliance depends on aneurysm size and

elastic fragmentation score; d) whether aortic regurgitation presence and severity is related to the diameter of sinusal (AoS) or tubular portion (AoT) of aorta and if aortic valve replacement accounts for a hemodynamic benefit (reduction of end-diastolic volume EDV).
Design: Patients who underwent to ascending aorta replacement for AAA between 2001 and 2010, with or without aortic valve replacement, were included. Clinical, echocardiographic, surgical and histological data were retrospectively reviewed. At histology, we searched for: atherosclerotic, inflammatory and degenerative (elastic fragmentation and cystic medionecrosis) substrate. The latter was evaluated using the semiquantitative method by Larson and Edwards (score 1-4).
Results: 222 patients (mean age 60.9±13.1 yrs; 174 M, 78.4%) were enrolled, subdivided in 7 groups: arterial hypertension (n=95, 43.2%), bicuspid aortic valve (n=46, 20.7%), atherosclerosis (n=29, 13%), aortitis (n=10, 4.5%), previous aortotomy (n=8, 3.6%), Marfan syndrome (n=5, 2.25%), idiopathic aneurysms (n=29, 13%). The aortic valve was replaced in 144 patients (64.9%). The highest AoS diameter was observed in previous aortotomy (5.12 cm), while the highest AoT diameter in aortitis (5.65 cm). The AoS diameter positively correlated with the elastic fragmentation score ($p<0.025$), unlike the AoT diameter ($p=0.336$). Age directly correlated with the elastic fragmentation score ($p<0.0001$). The elastic fragmentation score was higher in patients with Marfan and aortitis (<0.001). Aortic compliance correlated with the elastic fragmentation score ($p=0.017$). In 135 patients with aortic regurgitation, the correlation between incompetence severity and AoS size was statistically significant ($p=0.01$). In patients with aortic valve replacement, the difference between median pre- and post-operative EDV is statistically significant ($p<0.01$).
Conclusions: The disease entity underlying AAA is variable, with hypertension being the most prevalent risk factor (43.2%). As age increases, the degree of elastic fragmentation also increases, regardless of the underlying etiology. The most severe degree of elastic fragmentation was observed in Marfan syndrome and aortitis. With increasing elastic fragmentation score, higher AoS and AoT diameters and lower aortic compliance are observed.

325 Sudden Cardiac Death in the Young: Are There Gender Differences in Cardiovascular Causes?

S Rizzo, K Pilichou, E Carturan, G Thiene, C Basso. University of Padua, Padua, Italy.
Background: Sudden cardiac death (SCD) in the young is due to a wide spectrum of cardiovascular causes but few studies specifically addressed their prevalence and characteristics in the female (F) vs. male (M) gender.
Design: In the time interval 1980-2011, 591 SCDs in young people aged 1-40 yrs (mean age 25±9 yrs) have been prospectively studied according to a uniform pathology protocol in our referral pathology Centre.
Results: They were 406 M (69%) and 185 F (31%), mean age 26±8 vs. 24±10, $p=0.01$. Major causes included atherosclerotic coronary artery disease (CAD 108, 18%), myocarditis (72, 12%), arrhythmogenic right ventricular cardiomyopathy (ARVC 58, 10%), hypertrophic cardiomyopathy (HCM 55, 9%), dilated cardiomyopathy (22, 4%), non ath-CAD (41, 7%) and mitral valve prolapse (MVP 45, 7.5%). In 37 cases SCD was mechanical (6%) and in 101 (17%) the heart was structurally normal ("unexplained SCD"). Among cardiomyopathies, myocarditis, HCM and DCM show an almost equal prevalence in M and F (11%, 10% and 4% vs. 15%, 7% and 3.5%, respectively, p=NS). Atherosclerotic CAD (24% vs. 6%) and ARVC (13% vs. 3%) are the leading causes in M SCD victims. On the contrary, spontaneous coronary artery dissection (5% vs. 0.2%), MVP (14% vs. 5%) and mechanical causes (9% vs. 5%) are more typical of F SCD victims. SCD remains unexplained in 25% of F vs. 13.5% of M. Competitive sport activity is more frequent in M than F (17% vs. 3%). All p are statistically significant. Among F cases aged ≥18 yrs, 12% died suddenly during pregnancy or in the peri-partum period.
Conclusions: One third of young SCD victims are women. In the F gender, SCD remains unexplained in one forth of cases and major cardiovascular causes are represented by subtle substrates such as myocarditis and MVP. Athletic activity is underrepresented as compared to M, possibly explaining the low prevalence of ARVC among F SCD victims at difference from other inherited cardiomyopathies.

326 Intercalated Disc Ultrastructural Abnormalities Precede Histopathologic Changes in Desmoglein2 Transgenic Mice and Are Associated with Conduction Slowing and Inducible Arrhythmias

S Rizzo, EM Lodder, AO Verkerk, R Wolswinkel, L Beekman, K Pilichou, C Basso, CA Remme, G Thiene, CR Bezzina. University of Padua, Padua, Italy; Academic Medical Center, University of Amsterdam, Amsterdam, Netherlands.
Background: We sought to evaluate the pathological substrate of electrical instability in the pre-phenotypic stage of arrhythmogenic cardiomyopathy (AC), before myocardial cell death and fibro-fatty replacement onset.
Design: We studied transgenic mice carrying mutation of desmoglein2 (dsg2) in the adhesive extracellular domain (Tg-NS). Gross, histological and ultrastructural analyses were used in the pre-phenotypic stage of the diseases, i.e., between 2 and 6 weeks. The structure and molecular composition of the ID was assessed by electron microscopy (EM) and by immunofluorescence. Mice with cardiac over expression of wild-type dsg2 (Tg-WT) and wild-type mice served as controls. Surface ECGs, electrical epicardial mapping and patch-clamp experiments were performed to determine ventricular conduction and arrhythmia susceptibility.
Results: At gross and histologic examination, Tg-NS hearts appeared normal, with no evidence of replacement-type fibrosis. Immunofluorescence uncovered no differences in the level and localization of junctional proteins between Tg-NS/L mice and controls. Ultrastructural examination of the myocardium ruled out cardiomyopathic changes, including cell necrosis, focal myofibrillar lysis, dilated sarcoplasmatic reticulum and T-tubules, and mitochondrial clustering at this age. Widening of the intercellular spaces at the level of desmosomes/adherens junctions was seen in otherwise morphologically normal cardiomyocytes in 25% of TgNS at 2 weeks and in 100% at 6 weeks and the percentage of widened cellular junctions increased with age (from about 10% at an age of 2 weeks to 60% at 6 weeks). Morphometric analysis showed that the intercellular space was significantly widened in Tg-NS/L mice (149 ± 80 nm) compared with controls (32 ± 3.5nm), $p<0.05$. None of the control mice (Tg-WT, WT) displayed any intercellular space widening. QRS-prolongation and inducible ventricular arrhythmias were observed in mutant mice. A reduced action potential (AP) upstroke velocity due to a lower Na(+) current density was also observed at this stage of the disease.
Conclusions: *Dsg-2* mutant mice display ultrastructural evidence of desmosomes /adherens junctions widening, before development of cardiomyopathic changes. This coincided with conduction slowing and inducible ventricular arrhythmias thus emphasizing the importance of ID integrity for proper electrical conduction.

327 *JAZF1/PHF1* Rearrangement in Primary Ossifying Sarcomas of the Heart: A Novel Gene Fusion

JK Schoolmeester, AL Folpe, WR Sukov, JC Hodge, JJ Maleszewski. Mayo Clinic, Rochester, MN.
Background: Primary cardiac sarcomas represent a diverse group of malignancies, the majority of which lack recurrent translocations. Of the described translocation-associated cardiac sarcomas, synovial sarcoma is most common, with isolated reported cases of infantile fibrosarcoma, alveolar soft part sarcoma and low-grade fibromyxoid sarcoma.
Design: As part of a clinical validation for break apart strategy *JAZF1* and *PHF1* fluorescence in situ hybridization (FISH) probes, we identified a pulmonary metastasis that showed rearrangement of both loci. This lesion was from an unusual, distinctive ossifying cardiac sarcoma. Retrospective review of institutional cardiac sarcomas with ossification identified two additional cases. Histologic sections from all three cases were reviewed and corresponding formalin-fixed, paraffin-embedded tissue was tested for *JAZF1* and *PHF1* gene rearrangements. Cases showing rearrangement of both were then tested for *JAZF1/PHF1* fusion using a dual-color, double fusion FISH probe.
Results: The tumors occurred in 1 man and 2 women, with age at presentation ranging from 59 to 70 years (mean 65.6 years). Tumors arose in the inferoseptal left and right ventricles (1 case) and left atrium (2 cases) and ranged from 6.8 to 10.0 cm (mean 8.3 cm). The tumor from the original patient showed a distinctive morphology including monomorphic cells, nuclear palisading and ossifying "amianthoid fiber-like" collagen. FISH confirmed *JAZF1* and *PHF1* gene rearrangements and *JAZF1/PHF1* fusion. The remaining 2 cases showed a more pleomorphic infiltrate with areas of ossification, consistent with osteogenic sarcoma of the heart. These tumors were negative for *JAZF1* and *PHF1* rearrangements. All patients died of disease.
Conclusions: To the best of our knowledge, this represents the first example of a non-endometrial stromal neoplasm demonstrating a *JAZF1* gene rearrangement. Given the patient's male sex, the tumor's distinctive morphology, the presence of a *JAZF1/PHF1* gene fusion, and the absence of similar rearrangements in conventional cardiac osteosarcomas, this may represent a new entity among cardiac sarcomas, however confirmation of this hypothesis requires evaluation of additional similar cases.

328 The Activation of mTOR Pathway, a Marker of Endothelial Cell Involvement, Is Correlated with Antibody Mediated Rejection

M Tible, A Loupy, J-P Duong, P Bruneval. PARCC, Paris, France; Hopital Europeen Georges Pompidou, Paris, France.
Background: In cardiac transplantation, the pathological classification of the antibody mediated rejection (AMR) on endomyocardial biopsies (EMB) is based on histology (microvascular inflammation) and immunohistochemistry (deposition of C4d and/or CD68-positive intravascular macrophages). It is ranked in 4 grades, from pAMR0 to pAMR3. pAMR1 which corresponds to a suspicious AMR is divided in two categories: pAMR1(H+) based on histology findings alone and pAMR1(I+) based on immunopathologic findings alone. Previous studies suggested that mTOR pathway activation, detected by in situ microvascular expression of mTOR targets p70 S6 kinase (p70S6K) and phospho-S6 ribosomal protein (pS6RP), could be associated with endothelial cell involvement during AMR. The aim of the study was tocorrelate pS6RP and p70S6K expression with other AMR markers (C4d deposition, CD68-positive intravascular macrophages, and DSA); To assess the diagnostic value of immunohistochemical detection of pS6RP and p70S6K in microvessels of EMB.
Design: 280 protocol EMB harvested during a 1 year period of time in a single institution were used. 37 EMB with pathological features of AMR were included in the pAMR+ group encompassing 27 pAMR1(H+), 1 pAMR(I+), and 9 pAMR2. 37 EMB were randomly selected among the pAMR0 EMB and were included in the control group. Capillary expression of pS6RP and p70S6K was assessed by immunohistochemistry and ranked from grade 0 to grade 4. Only grades 3 and 4 were considered as positive. In parallel DSA were assessed using Luminex technique.
Results: In the pAMR+ group, pS6RP and p70S6K were expressed in the endothelial cells of the EMB ranked pAMR2 (4/9 and 7/9 respectively), and also in grade pAMR1(H+) EMB (3/27 and 10/27 respectively). In the control group 1/37 EMB was positive. Microvascular expression of pS6RP and p70pS6K was correlated with DSA ($p<0.01$) and microvascular inflammation ($p<0.05$).
Conclusions: The endothelial expression of mTOR targets pS6RP et p70S6K, markers of endothelial cell activation, is associated with AMR in both definite AMR grade pAMR2 and suspicious AMR grade pAMR1(H+), negative for C4d and CD68. That latter finding underscores the diagnostic value of pS6RP and p70S6K immunohistochemistry to characterize AMR in C4d-negative EMB.

329 Lymphoplasmacytic Response to Atheroma Mimicking Vasculitis

AD Treacy, K Norita, PJ Ingram, MN Sheppard. National Heart and Lung Institute at the Royal Brompton Hospital, London, United Kingdom; Institute of Forensic Medicine, Belfast, United Kingdom.

Background: Coronary artery atheroma accounts for the vast majority of sudden cardiac deaths whilst coronary artery vasculitis accounts for a rare number. We report a series of atheromatous coronary arteries with associated florid lymphoplasmacytic inflammation mimicking vasculitis.

Design: Three cases with mass like lesions surrounding atheromatous coronary arteries were referred from a single centre to the National Heart and Lung Institute at the Royal Brompton Hospital for expert pathology review. The cases were from males with mean age 74 years (range 55 – 91). In all cases coronial autopsies were carried out for sudden deaths in the community. Past medical histories of note were hypertension (N=2) and ischaemic heart disease (N=1), with one patient having a past history of aortic aneurysm repair.

Results: At autopsy, firm, white and whorled masses were described surrounding atheromatous coronary arteries ranging in size from 9-25mm in diameter. Each coronary artery had intimal atheroma ranging from moderate to severe. A thrombus was identified in one case. No gross infiltration of the myocardium was seen. No vascular abnormalities or lesions were identified elsewhere. Histological sections showed a mixed inflammatory infiltrate extending from the media into the adventitia, composed predominantly of plasma cells and lymphocytes with rare neutrophils and eosinophils. No giant cells or epithelioid cells were noted. No necrosis was present. There was focal infiltration of the myocardium by lymphoid aggregates. There was accompanying dense fibrosis accounting for 50% of the mass size. The presence of intimal circumferential atheroma was confirmed in all cases. Myocardial fibrosis was identified in one case. No inflammatory infiltrate was present in the myocardium. Slides from all three cases were stained with IgG and IgG4 by immunohistochemistry. The stained cells were counted in three high power fields from areas with the highest density of plasma cells using a 40x objective and 10x eyepiece of an Leica microscope. The proportion of IgG4 expressing plasma cells was greater than 50% of IgG-expressing cells in two of the three cases.

Conclusions: Atheroma may be associated with mild chronic inflammation present in the intima or associated with plaques. IgG4 related disease has been described in various organ sites, we report a series of IgG4 related coronary artery vascular lesions in association with atheroma.

330 Collagen Alterations in the Dissecting Aortic Aneurysm (DAA) Caused by N-(2-Aminoethyl) Ethanolamine (AEEA) in Rat

Y Xu, G Vargas, PJ Boor. University of Texas Medical Branch, Galveston, TX.

Background: The industrial chemical N-(2-aminoethyl) ethanolamine (AEEA) induces dissecting aortic aneurysm (DAA) in newborn rats following *in utero* exposure. To extend our knowledge about the severe deleterious effects of AEEA on normal vascular development, we aim to study the extracellular matrix changes during the formation of developmental DAA.

Design: We treated pregnant Sprague-Dawley rat dams with AEEA by gavage on gestation day (GD) 14-20, a period of rapid aortic development (Doses: 10, 50, 100 and 150 mg/kg/day; controls received saline only). Aortas from fetuses on GD 20 and from newborn pups (day 1) were examined by histopathology. Total collagen in aorta of fetuses from dam treated with AEEA (150 mg/kg/day) was examined by multiphoton fluorescence (MPF) and second harmonic generation (SHG) microscopy. Collagen types 1 & 3 distribution and quantization in aorta were further studied by immunohistochemistry and native western blot respectively.

Results: GD 20 fetuses showed no lesions. Extensive DAA was found in 100% of newborn pups (post natal day 1) in the two highest dose groups (100 and 150 mg/kg/day). Mediastinal hemorrhage, dissection in pulmonary artery and carotid artery were also found. A lesion grading system was devised; a dose-reponse was demonstrated for severity of lesion grade with AEEA dosage. Multiphoton fluorescence (MPF) and second harmonic generation (SHG) microscopy showed total collagen in aorta of GD 20 fetuses from treated dams was decreased. GD 20 fetuses from treated dams showed a decreased content of medial and adventitial collagen types 1 & 3 in aorta by immunohistochemistry; this decrease was confirmed by native western blot in pooled aortas. Collagen types 1 & 3 in AEEA treated group significantly decreased 34% and 30% respectively. There was no significant change of collagen types 1 & 3 of skin in AEEA treated group compared to the control, indictating that the collagen pathophysiology induced by AEEA exposure is specific for aorta and not a generalized phenomenon.

Conclusions: The pathologic mechanism of AEEA induced developmental DAA may be related to decreased collagen types 1 & 3 weakening the vascular wall. DAA induced by AEEA is a reproducible model that is useful to study the underlying mechanisms of DAA development *in vivo.*

331 Incidental Ascending Aortitis: The Histologic and Clinical Spectrum

L Xu, L Goicochea, F Tavora, A Burke. University of Maryland Medical Center, Baltimore, MD; Messejana Heart and Lung Hospital, Fortaleza, CE, Brazil.

Background: The incidence of aortitis in series of aortic aneurysm repair is between 5 and 8%. In most cases, the diagnosis is made initially by histopathologic evaluation of the specimen. There are few single-institution clinicopathologic series of aortitis.

Design: We prospectively studied histologic features of aortitis in series of repaired aortic aneurysms over a 6-year period with clinical correlation and follow-up.

Results: Of 254 aortic resections, there were 17 cases of incidental aortitis (6.7%); 9 women (74 ± 13 years) and 8 men (62 ± 15 years). 4 patients had prior autoimmune disease (rheumatoid arthritis, giant cell arteritis, ankylosing spondylitis, and IgA nephropathy); 1 was diagnosed subsequently with Takayasu disease. Additional 3 patients had positive rheumatoid factor and ANA, history of Lyme disease, and fibromyalgia. Grossly, all cases of aortitis showed a distinct wrinkled intima. The surgeon noted abnormal thickened aortic wall intraoperatively in 8 cases. Histologically, there were two types of aortitis: necrotizing aortitis and periaortitis. Necrotizing aortitis demonstrated three phases: acute, healing, and healed. In the acute phase (n=3), there were linear zones of necrosis > 3 mm with peripheral predominately adventitial macrophage giant cells; 2 cases also showed pockets of neutrophils. In the healing phase (n=5), there was both zonal medial necrosis < 3 mm with surrounding granulomatous reaction, and areas of healing with smooth muscle cell proliferation, often with proteoglycans mimicking cystic medial degeneration. In the healed phase (n=7), only the latter changes were noted. All cases showed brisk adventitial chronic inflammation and scattered inflammatory infiltrates around medial vessels. The two cases of periaortitis had numerous (>25 per hpf) IgG4 plasma cells and adventitial fibrosis. Intimal and adventitial thickening was mild in necrotizing aortitis (mean 0.6 and 0.9 mm, respectively) and greater in IgG4 disease (mean 4.2 and 1.3 mm, respectively). 2 patients with necrotizing aortitis progressed with new descending aortic aneurysms. One of these patients was treated with immunosuppressive treatment and one with anti-inflammatory drugs; they were the only patients given systemic treatment.

Conclusions: Aortitis is the cause of about 7% of surgically repaired ascending aortic aneurysms. Most cases show necrotizing medial inflammation that heals with a characteristic histologic appearance. IgG4 disease is a less common cause of aortitis that involves primarily the adventitia.

332 Hypersensitivity Myocarditis before Heart Transplantation Is Associated with Increased Acute Cellular Rejection after Transplantation

SK Yoshizawa, TS Kato, D Mancini, CC Marboe. Columbia University Medical Center and the New York Presbyterian Hospital, New York, NY.

Background: Hypersensitivity myocarditis (HSM) is associated with the use of multiple drugs, and has been occasionally observed in the patients with end-stage heart failure. However, whether or not HSM at the time of heart transplantation (HTx) affects long-term prognosis including acute cellular rejection (ACR) and antibody-mediated rejection (AMR) after HTx remains unclear. This study addresses the occurrence, clinical and pathological characteristics, and prognosis of patients with HSM at HTx.

Design: 766 consecutive patients who underwent de-novo HTx at Columbia University Medical Center between 2000 and 2010 were retrospectively reviewed. Clinical characteristics and pathological findings of patients with pre-HTx HSM diagnosed by histological evaluation of the explanted heart were analyzed. Prognosis after HTx was compared between the patients with or without HSM.

Results: HSM was observed in 21 patients (2.7%). The rate of pre-HTx HSM in our hospital has been decreasing during the study period in inverse relation to the rate of left ventricular assist device implantation before transplant. 19 patients (90%) had peripheral blood eosinophilia at the time of HTx, but in no case was HSM clinically diagnosed. Dobutamine, a common cause of HSM, was administrated in 12 patients (57%). All patients had varying degrees of mixed inflammatory infiltrates with eosinophils, lymphocyte, macrophages, and plasma cells, but none of the patients showed myocardial necrosis. The number of episodes of biopsy diagnosed ACR (ISHLT grade ≥2R) was 11 (3.9%) in HSM patients and 197 (2.2%) in patients without HSM (p=0.06) during the first year post-HTx, and 11 (3.8%) in HSM patients and 78 (1.5%) in patients without HSM (p=0.006) after second year post-HTx. Regarding AMR, there was no statistically significant difference between the groups throughout the study period. Post-transplant survival did not differ in patients with or without pre-transplant HSM.

Conclusions: HSM at the time of HTx is associated with an increased frequency of late ACR after HTx. Post-HTx survival is not influenced by pre-transplant HSM.

Cytopathology

333 Intra-Abdominal Neuroendocrine Tumor Diagnosed by Endoscopic Ultrasound-Guided Fine Needle Aspiration (EUS-FNA): A Retrospective Study from an Academic Tertiary Center

R Albadine, G Soucy, AV Sahai, SC Paquin, G Gariepy. Centre Hospitalier Universitaire de Montréal, Montréal, QC, Canada.

Background: Neoplastic lesions of the pancreas, liver, retroperitoneal lymph nodes can be better visualized and appropriately sampled with fine-needle aspiration biopsy by endoscopic ultrasound (EUS-FNA). Diagnosis of pancreatic endocrine tumor can be rendered, in most cases, without difficulty based on cytomorphologic and immunophenotypic features. This study reviews the usefulness and accuracy of EUS-FNA in the diagnosis of neuroendocrine tumor (NET) in pancreas, liver, and lymph nodes.

Design: This is a retrospective study. Intra-abdominal EUS-FNA specimens (2003-2012) with a NET were retrieved. Metastatic small cell carcinoma was excluded. Immunohistochemistry study (small panel: CD57, CD56, synaptophysin, chromogranin A and B) was performed when cell block was available. Cases were classified as consistent with NET, possible/suggestive of NET, few cells with neuroendocrine differentiation. Clinicopathologic data were collected. On site cytopatholgic evaluation was done in all cases.

Results: We retrieved 148 patient specimens. Overall accuracy of EUS-FNA compared to definitive histopathology of surgical specimen was 85% (81/95). In 14 cases, there was little discrepancy. Final diagnosis was: Paragangliomas (3 cases); 1 intra pancreatic and 2 retroperitoneal; composite carcinoma with ductal, acinar, endocrine components (5 cases); Schwannoma (1 case); Metastasis from acinar cell carcinoma (1 case); Solid